Potentialities of Dynamic Breast Thermography

Amina Amri, Anthony James Wilkinson and Susan Helen Pulko

Abstract Since the introduction of breast thermography into medicine, researchers have been interested in enhancing the thermal contrast in thermograms taken at steady state. It was found that cooling the surface of the skin during long acclimation periods produced better thermal contrast, although it was agreed that acclimation periods of up to 15 min may suffice to reflect functionalities of inner skin tissues. However, the use of artificial sources for cooling the skin has revealed new functional information that complements steady state thermography findings. The method has been referred to as 'Dynamic thermography' and is based on monitoring skin's thermal state after cold stress. Although dynamic thermography showed some promises in breast cancer diagnosis during the 70s, it has not received much interest till the advent of computer image processing techniques. Analytical tools such as sequential thermography, subtraction thermography, μ-thermography and thermal parametric images have been used in order to increase the accuracy of breast thermography. Other processing techniques used thermal transients of control points on the breasts to examine the change in blood perfusion induced by the presence of a breast disease. Autonomic cold challenge has also been used to identify a tumour's blood vessels. Recent numerical methods have investigated the effectiveness of dynamic breast thermography and revealed new parameters that are strongly correlated with tumour's depth. Here we review the state of the art in dynamic thermography as it is applied to breast diagnosis and identify some of the potential information that could be provided about breast diseases.

Keywords Breast cancer · Cold stress · Autonomic cold challenge · Subtraction thermography · Sequential thermography · μ-thermography · Dynamic thermography · Thermal recovery models

A. Amri (✉) · A.J. Wilkinson · S.H. Pulko
University of Hull, Hull, UK
e-mail: amri.amina@gmail.com

1   The Concept of Dynamic Thermography

Breast thermography was introduced into medicine by Lawson [1] who observed that some breast cancers cause a rise in the temperature of the overlying tissue and argued that breast cancers could be detected at an early stage if thermal scan of the chest could be performed. Since then medical research has focused on the development of medical infrared scanning systems that could produce a quantitative temperature map of the breast [2, 3]. This interest in infrared scanning systems has been driven by the potential value of thermograms and was encouraged by the development of sensitive infrared detectors and sophisticated scanning systems for military requirements. Discussion about spurious thermography findings and possible errors that could affect thermal images have pointed out the importance of insuring that the temperatures measured at the surface of the skin are relevant to the physiological or pathological conditions of the body and not caused by artefacts [2–5]. It has been thus agreed that thermography should be performed using protocols during which thermal images of the unclothed part of the body be taken after 10–15 min acclimation period in a room of temperature between 18 and 24 °C, free of drafts, heat sinks or sources and that the patient be seated in an appropriate position. Under the foregoing conditions, better thermal contrasts have been observed. Further, faster scanning techniques and better thermal resolution are required for accurate thermal mapping.

At this stage, it was known that, in a healthy body any two symmetrically located areas of skin are at the same temperature under controlled environmental conditions [6–9]. Therefore, it was important to be able to correlate thermal contrast observed on thermograms with pathological conditions of the body in order to appraise the clinical value of thermography and to avoid subjective interpretation of thermograms. Barnes [5] has observed that the contrasts shown on thermograms are essentially caused by the generators of heat within the body and that thermograms can give information about pathological conditions from which the patient may be suffering. Subsequently, Williams [8, 9] proposed several causes for thermal contrast and stated that a range of breast diseases such as abscesses and some tumours induce a hot spot on the surface of a thermogram.

In the light of this, it was desirable to enhance the thermal contrast observed on thermograms given that the temperature of the skin is affected by environmental parameters and inner tissues characteristics. Barnes [10] demonstrated that the acclimation period is nothing but natural cooling of the skin and observed that better thermal contrasts are associated with longer acclimation periods which allow an equilibrium condition to be reached. Using the Barnes Mod I infrared scanner, a modified infrared instrument originally designed for military applications [11], Barnes [10] obtained a series of thermograms during natural cooling of the unclothed upper body of a patient in a room temperature of 29 °C and observed that the contrast was progressively increased after 15, 42, 65 and 94 min acclimation period while thermal details were still faithfully reproduced. In another experiment, Barnes [10] artificially cooled an arm by placing a damp towel on it for a few

seconds and then drying it quickly. A series of thermograms were taken during 27 min thermal recovery period at 3 min interval. An enhancement of contrast was observed during the first 9 min after which contrast decreased as the arm returned to thermal equilibrium.

Although heating the skin would obviously decrease the thermal contrast, Barnes [10] examined the effect of heating the arm progressively from ambient up to a temperature of 43 °C. Thermograms taken at temperatures of approximately 34, 37, 40, 41, 42 and 43 °C showed that at approximately body temperature, thermal contrast disappear. At elevated temperatures, a different thermal pattern emerged including cool areas directly over the veins. Consequently, Barnes [10] concluded that heating the skin could provide information about thermal conductivities of various tissues beneath it and suggested the use of superficial heating to study dermatological problems.

Concurrently, Williams [9] also reported that thermal contrast is accentuated by longer acclimation periods and by overcooling using artificial means. A steady state thermogram of a patient with advanced carcinoma of the right breast showed a temperature difference of 3.5 °C. When the chest wall was cooled using a towel soaked in iced water, the thermal contrast was observed to increase. The enhancement observed in the thermal contrast over a cancerous breast has marked the beginning of the use of superficial cooling as part of breast thermography protocols.

The advent of thermography as an adjunct technique for breast screening has spurred many medical researchers to establish its value in breast diseases with regard to known modalities of mammography and physical examination. Amalric et al. [12] compared thermography with physical examination, mammography and cytology. During thermography examination, the patient's chest was sprayed with a cooling liquid which was evaporated using a fan for 10 min. Thermograms were taken just after cooling. Thermographic findings were then compared with histological findings for evaluating thermographic usefulness. Out of 1879 confirmed cancers, 9% could not been identified either by physical examination or by mammography, but have been detected by the combination of cold stress and thermography.

2   Breast Dynamic Thermography Using Autonomic Cold Challenge

The early 80s witnessed the use of a protocol involving autonomic challenge before thermography. The method involved cooling of the extremities (hands or feet) by ice water immersion as part of breast thermography protocol. The cold challenge has been known as a test of sympathetic function and was used as a definitive diagnostic method for Complex Regional Pain Syndrome also known as Reflex Sympathetic Dystrophy (CRPS/RSD). The introduction of an autonomic challenge

was predicated on the fact that at some stage of its growth, cancerous tumours release angiogenic growth factor proteins that stimulate blood vessels to grow into the tumour, so that it can be supplied with nutrients and oxygen. However, angiogenesis growth does not continue throughout all stages of cancer. The autonomic cold test was intended to identify the development of a tumour's blood new vessels known as neoangiogenesis, and these could then be correlated with the development and existence of breast cancer. Since neoangiogenesis are devoid of a muscular layer and normal neural regulation, they would fail to constrict in response to a sympathetic stimulus. Therefore, a high blood perfusion rate is maintained in the tumour region as well as a high level of metabolic heat generation, while vasoconstriction occurs near the skin surface.

The concept was initiated in France where Gautherie et al. [13] used hand immersion in an attempt to make breast thermography more sensitive. The study used large sample data including over 10,000 patients. Thermograms could be taken prior to and after 45 s of cooling. It was reported that false positive rate decreased to 3.5%.

However, there have been theoretical claims that some anatomical factors can compromise the ability of the sympathetic nervous system to provoke vasoconstriction. Cockburn [14] argued that dilated vessels or capillary networks that resulted from surgery, incisional biopsy and lumpectomy, as well as local trauma and thoracic spine instabilities, would fail to respond to the autonomic cold challenge thus compromising the detection of tumour's neoangiogenesis. He also suggested that patient's own anxiety about the procedure may cause a sympathetic fight or flight response before the autonomic cold challenge and may lead to negative findings after applying cold stress. Therefore, researchers in the realm of breast thermography discontinued the use of the autonomic cold challenge in the early 90s after observing poor correlation between the results using cold stress and medical case histories [14–16].

Using advanced medical imaging systems, Amalu [17] has conducted a clinical study in order to reappraise the role of autonomic cold challenge as it might be applied to breast thermography. Breast thermograms of 23 patients with histologically confirmed breast cancers demonstrated positive and negative responses to cold stress. Amalu [17] found that excluding the autonomic cold test from breast thermography protocol does not affect the sensitivity or the specificity of thermography in the detection of breast cancers and concluded that more studies are needed to assess the validity of the autonomic cold test.

3   Characterisation of Thermal Recovery After Cold Stress

Barnes' observations during thermal recovery from superficial cooling and heating stimulated the interest of Japanese medical researchers to obtain information about the reaction of blood perfusion, metabolic heat generation and thermal conduction of the human skin to superficial stimulus. Nagasawa and Okada [18] referred to this

type of thermography as "dynamic thermography" because it is based on recording thermal transient during the dynamic thermal recovery of the skin.

Nagasawa and Okada [18] devised a spot cooling source consisting of a piece of ice in a film container of 30 mm diameter. A constant pressure of about 200 g insured that the cooling source was kept in contact with the skin. The part of the skin in contact with the device beyond the cooling area was insulated. Instead of taking several thermograms of the cooled area at different time intervals during thermal recovery, Nagasawa and Okada [18] recorded the thermal transient at the centre of the cooled area in a room that fulfilled thermography conditions. After cooling a pair of healthy human cheeks for 15 s, the thermal recovery curve of the right cheek was almost identical to the left cheek. After removal of the coolant, the temperature T of the centre of the spot recovered rapidly for the first minute and then its rise became more gradual ultimately reaching thermal equilibrium temperature, T_∞, which was almost the same as before cooling. The time needed to reach the final temperature was referred to as Recovery Time, ReT.

In order to calculate ReT, the thermal recovery curve was processed to a straight line using a logarithmic transformation of the difference between T and T_∞. The calculated and the measured values of ReT were found to be almost identical. The recovery time, ReT, was measured in cases of various diseases. In a case of hemangioma, ReT value of 3 min suggests active blood perfusion whilst for lipoma, the ReT was longer suggesting a low heat activity. Recovery time measurements were also used to track the acceptance of transplanted tissue in a deficient region on the cheek. It was found that after the first 20 days the recovery time was relatively slow but became faster after 80 days, which indicated its acceptance. Consequently, it was concluded that ReT depends on the kind of disease and its seriousness. Nagasawa and Okada [18] further investigated the value of dynamic thermography in observing the process of diseases and the effects of medication. Figure 1 shows a comparison of the linearized thermal recovery curves of a postoperative inflammation area, after removing an impacted mandibular third molar, and its
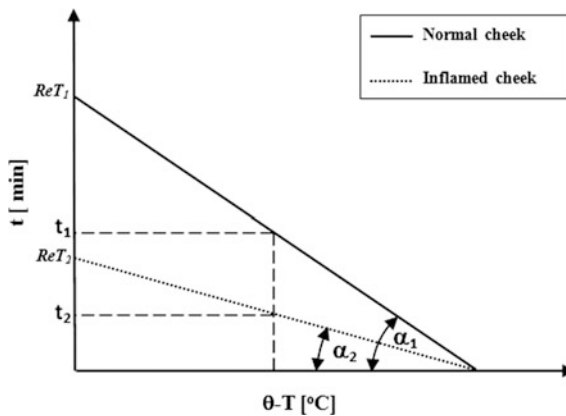

Fig. 1 Linear representation of thermal recovery curves of normal and inflamed cheeks after cooling [18]. The ratio $RtR = t_2/t_1 = \tan\alpha_2/\tan\alpha_1 = ReT_2/ReT_1$

symmetrical part. It was observed that the ratio of their corresponding slopes was equal to the ratio of their recovery times. This ratio was referred to as Recovery time Rate, *RtR*, and was used to observe the gradual recovery of the inflammation.

After examining various clinical experiments of dynamic thermography using cooling as well as heating stimuli, Nagasawa and Okada [18] concluded that a thermal recovery process could provide quantitative information about blood perfusion and heat activity of a tumour and that dynamic thermography could be applicable to differential diagnosis. It was also suggested that chemicals may be used as a stimulus for dynamic thermography in order to observe the reaction of specific diseases.

Concurrently with the clinical work of Nagasawa and Okada [18], Cary and Mikic [19] described a localised cooling method that could be used in differential diagnosis of human tumours. Although it was already known that thermal contrast is enhanced by cooling, the observed effects of cooling were not well understood at the time of the study. The method was established using the fact that the growth of tumours is usually associated with increases in the local blood perfusion and the local metabolic rate. These changes can produce an effect on skin temperature maps in the region above a tumour. Therefore, differential diagnosis of tumours could be made from comparison of temperature fields near tumours and in the corresponding region of the contralateral breast, on the basis that this is healthy tissue. Further, it was assumed that blood perfusion rates in healthy or normal tissue could differ significantly from blood perfusion rates through tumours during moderate cooling. Blood rate differences between cancerous and healthy tissue are thereby reflected in the observed thermal contrast.

The theoretical concept was later used to devise a simple, inexpensive local cooling system that could help in differential diagnosis of breast tumours [20]. The system comprises two cylindrical cooling units weighting approximately 500 g each. The units are filled with crushed ice at least 30 min prior to testing so that the cooling disk reaches 10 °C or less. The patient should be lying on her back with pen marks on the point where the tumour is closest to the surface. During a 10 min test, the units are held by the patient on the region of interest and on its symmetrical healthy part. Each unit insures a small surface cooling area of approximately 25 mm around which the skin in contact with the cooling device is insulated. Using such a system, relatively large temperature differences between the skin over cancerous tissue and that above healthy tissue could be obtained, without the heat loss from the patient being sufficient to affect patient comfort adversely and so limit the enhancement of the thermal contrast. The cooling units insure controlled cooling as well as recording the temperature of the cooling surface at one minute intervals. It was observed that thermal equilibrium was reached after 10 min and the thermal contrast ΔT after 10 min was calculated.

During cooling, the rate of variation of skin temperature T_s with time is influenced by blood perfusion of the tissue. When the temperature of a tissue does not vary significantly in space during cooling because of the inner fixed body temperature, the rate of variation of T_s could be expressed as:

$$\frac{dT_s}{dt} \propto \omega_b(T_a - T_s) \tag{3.1}$$

where ω_b is the blood perfusion rate and T_a is the temperature of the arterial blood perfusing the tissue. However, the rate of variation of T_s is nonlinearly related to blood perfusion due to the complex breast tissue structure that causes both spatially- and time-varying temperature field. Since the ratio $(dT_s/dt)/(T_a - T_s)$ is a monotonically increasing function of perfusion rate, a parameter M was defined as:

$$M = \frac{dT_{s2}/dt(T_a - T_{s1})}{dT_{s1}/dt(T_a - T_{s2})} \tag{3.2}$$

To quantify the response of the local cooling device to known breast diseases, M and ΔT values were used to define diagnosis criteria. If $\Delta T \geq 0.9\ °C$ or $M \geq 1.35$ then the test was assumed positive for cancer. On the other hand, if $\Delta T < 0.9\ °C$ and $M > 1.35$ then the tumour was classified as non-malignant. The local cooling method was tested on 130 women for whom xerographical, thermographical, clinical and pathological information was available. Fifty-two of the women were normal. There were 31 carcinomas, 14 solitary cysts, 4 benign tumours and 22 diffuse dysplexia. Other patients include 5 women with asymmetrical axillary tail and 2 with abscesses or inflammation. Masses were of average diameter of 17 mm and were 15 mm deep.

The foregoing criteria correctly diagnosed: 23 of 31 malignancies, which corresponds to 74%; 16 of 18 benign growths, which is 88%, and 46 of 52 normal cases which is also 88%. However, 10 of 22 women (45%) who had asymmetrical diffuse non-malignant disease would have been falsely diagnosed as having cancer. Some false negative results were caused by clinically occult carcinomas with insignificant thermal contrast and by large necrotic, inactive neoplasm. On the other hand, false negative findings were induced by large thermal contrasts observed in benign breast diseases such as sclerosing adenosis, cystic disease, fibroadenoma and abscesses. Cary et al. [20] have outlined some technical issues in the cooling unit and procedure that could have influenced the results including unequal initial disc temperature, improper location of the unit during testing and movement of the units during testing due to patient's breathing.

4 A Mathematical Model for Thermal Recovery After Cooling

Since the early 60s, the medical community has been aware that steady state thermography could produce false positive as well as false negative findings. It was, therefore, important to investigate theoretically whether dynamic thermography

could provide substantial information which could be useful for the clinical diagnosis.

Motivated by the findings of Nagasawa and Okada [18] during thermal recovery after cold stress, Steketee [21] subjected the skin of the forehead of 20 healthy subjects to a cold temperature T_{cold} and subsequently recorded the thermal recovery over a period of 15 min. The recovery curve shown in Fig. 2a was approximated by a mono-exponential function:

$$T - T_{cold} = (T_{\infty} - T_{cold})(1 - e^{-\mu t}), \tag{4.1}$$

where T_{∞} is the steady state temperature. The value of the decay constant, μ, was determined from a semi-logarithmic plot of $T_{\infty} - T$ as a function of time as shown in Fig. 2b. However, it has been noticed that the steady state temperature T_{∞} was

Fig. 2 Typical curves obtained by Steketee and Van Der Hoek [22] after cooling the forehead. a Thermal recovery and b semi-logarithmic linearization of $T_{\infty} - T$ versus time
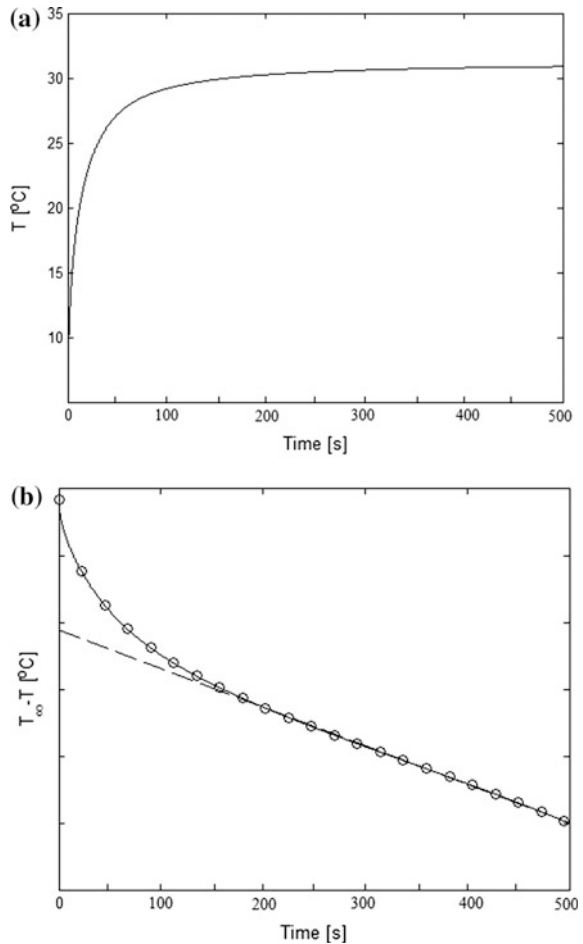
lower than the temperature before cooling inconsistent with the observation of Nagasawa and Okada [18] that T_∞ was approximately the same before cooling. Furthermore, data obtained using thermal recovery measurements taken over a shorter period, couldn't be fitted by a mono-exponential curve as shown in Fig. 2b. The variance of the measured decay constants was also very high. Therefore, Steketee and Van Der Hoek [22] used a theoretical model based on the bioheat equation attributed to Pennes [23] in order to understand the character of the thermal recovery and improve the method.

The following Pennes [23] bioheat equation was used to model heat transfer during thermal recovery:

$$\rho c \frac{\partial T}{\partial t} = k \frac{\partial^2 T}{\partial x^2} - \omega_b \rho_b c_b (T - T_a) + Q_m \qquad (4.2)$$

In Eq. (4.2), ρ (kg m^{-3}), k (W m^{-1} K^{-1}) and c (J kg^{-1} K^{-1}) denote the density, thermal conductivity, and specific heat capacity of tissue; ρ_b, c_b are density and specific heat capacity of blood; ω_b (s^{-1}) is the blood perfusion rate; Q_m is the metabolic heat generation; T_a is the supplying arterial blood temperature which is assumed constant, and T is the breast temperature.

A one-dimensional homogeneous skin model was used to study the thermal transient after cooling the surface at a temperature T_{cold}. Assuming that the skin is at body temperature, T_c, at a distance L from the surface and that the surface is exposed to ambient temperature, T_f, the following boundary conditions were prescribed

$$\begin{cases} k\frac{\partial T(x,t)}{\partial x}\Big|_{x=0} = h_0[T(0,t) - T_f] \\ T(x,t) = T_c \quad \text{for} \quad x \geq L \end{cases} \qquad (4.3)$$

In Eq. (4.3), h_0 is the effective heat transfer coefficient that combines the heat transfer attributable to convection and radiation as well as the cooling effect associated with evaporation. Defining $\theta = T - T_{cold}$, Eq. (4.2) becomes:

$$\frac{\partial \theta}{\partial t} = \alpha \frac{\partial^2 \theta}{\partial x^2} - \beta \theta + \gamma \qquad (4.4)$$

where α is the thermal diffusivity $\alpha = k/\rho c$, $\beta = \omega_b \rho_b c_b/\rho c$ and $\gamma = (Q_m/\rho c) + \beta \theta_c$. The boundary conditions then become:

$$\begin{cases} \frac{\partial \theta(x,t)}{\partial x}\Big|_{x=0} = h'[\theta(0,t) - \theta_f] \\ \theta(L,t) = 37 - T_{cold} \quad \text{for} \quad x \geq L \end{cases} \qquad (4.5)$$

where $h' = h_0/k$ (m^{-1}). Steketee and Van Der Hoek [22] solved the problem using the Laplace transformation method [24] and the complex inverse Bromiwich's integral formula [25] to obtain the thermal transient during recovery:

$$\theta(x,t) = \theta(x,0) + A \frac{\sinh \eta(L-x)}{\eta \cosh \eta L + h' \sinh \eta L}$$
$$- 2\alpha A \sum_{n=1}^{\infty} \frac{\exp(-\mu_n t) p_n^2 \sin p_n [1 - (x/L)]}{\mu_n L[p_n^2 + h'L(1 + h'\alpha)] \sin p_n} \tag{4.6}$$

where

$$A = \frac{\eta[\theta_c + (\gamma/\beta)(\cosh(L\eta) - 1)]}{\sinh(L\eta)} + h'\theta_f \quad \text{and} \quad \eta = \sqrt{\beta/\alpha}$$

$$\mu_n = \beta + \frac{\alpha p_n^2}{L^2}; \quad \tan p_n = -\frac{p_n}{h'L} \text{ and } \beta \neq 0$$

The surface temperature $\theta(0,t)$ and the steady state value $\theta(0,\infty)$ were derived from Eq. (4.6).

$$\theta(0,t) = 2\alpha A \sum_{n=1}^{\infty} \frac{[1 - \exp(-\mu_n t)] p_n^2}{\mu_n L[p_n^2 + h'L(1 + h'\alpha)]} \tag{4.7}$$

$$\theta(0,\infty) = A \frac{\sinh \eta(L)}{\eta \cosh \eta L + h' \sinh \eta L} \tag{4.8}$$

Equation (4.7) can be used to study the effect produced by a variety of parameters on the steady state temperature and to estimate the time needed to reach that temperature that Nagasawa and Okada [18] refer to as *ReT*. Equation (4.8) shows that T_∞ depends on the temperature at depth *L*. The later varies among subjects implying that T_∞ cannot be used as a reliable measurement for blood perfusion. Furthermore, the theoretical solution (4.6) showed that the decay constants, μ_n, depends strongly on the thermal diffusivity of the tissue. It was also concluded that a two-exponential model should be used to fit the thermal recovery curve in order to better discriminate normal and pathological blood circulation.

5   Computer Assisted Dynamic Breast Thermography

Computers were introduced for the qualitative analysis of breast thermograms in the 70s [26–29] with the aim of improving the accuracy of diagnosis. It was a reasonable assumption that a computer-based system would be a fast way of diagnosing abnormality, and would be less expensive than visual interpretation in a large breast screening program. Winter and Stein [28] assessed the ability of three computer image processing techniques: spatial signature analysis, symmetry measurement using thermal density distributions and image coding by contour map data structure. Newman et al. [26] devised a simple automated technique for obtaining

the breast outline and investigated criteria for abnormality. Ziskln et al. [29] classified 85 thermograms into normal and abnormal categories using a statistical decision program based on a linear discriminant analysis technique. They reported an overall accuracy of 85%.

Over the years, different methods of dynamic breast thermography have been reported. After the application of an external cold stress, thermal recovery of the breast could be examined by means of sequential thermograms taken at time intervals, or/and subtracting sequential thermograms to produce a single contrasted thermogram. Another approach was to compare the thermal transients of particular areas of interest on the abnormality with its contralateral symmetrical part.

Using a standardised cooling procedure, Geser et al. [30] reduced the temperature of the breast by approximately 3 °C using two fans. A computer-assisted discriminant analysis was used to classify a sequence of 20 thermograms recorded during thermal recovery of the breast after cooling. This quantitative dynamic thermography was then able to correctly classify 80% of 162 patients with negative clinical and mammography findings and 72.5% of 51 patients with proven breast cancer. When combined with steady state thermography, the false positive rate was reduced to 40%, though this value remains high.

Usuki et al. [31] combined observation of steady-state thermal maps with dynamic thermography after cold stress in a clinical study that included 56 breast carcinomas and 320 diagnosed benign diseases. Unspecified imaging procedures were used. Thermographic measurements were taken in a room of temperature 24 ± 1 °C and $60 \pm 10\%$ humidity using a thermo-tracer 6T66 (NEC-Sanei Co.). After an acclimation period of 15 min, steady state thermograms were taken. Soon after, the breasts were cooled with 70% alcohol mist and thermograms were taken at 0, 1, 2 and 3 min after cooling. Thermograms were then processed using imaging software that subtracted thermograms obtained immediately after cooling from the thermograms obtained 3 min after cooling. Statistical analysis of steady state thermography findings provides a sensitivity of 85.7%, a specificity of 65.6% and a total accuracy of 68.6%. In contrast, subtraction thermography showed a sensitivity of 89.3%, a specificity of 78.4% and a total accuracy of 80.1%. It was then concluded that, although subtraction thermography after cold stress decreases the false positive rate, it cannot be used as an ultimate breast imaging method. It was also recommended that correlations between steady state and subtraction thermography findings required more studies and that image analysis techniques needed further development in order to be used in this context.

Uchida et al. [32] developed a physiological functional image processing system for the quantitative analysis of sequential thermograms obtained during thermal recovery of the breast after cooling. This system used models developed by Steketee and Van Der Hoek [22] which describe the rewarming of the skin after cold stress is removed. By assuming that this thermal recovery can be approximated by a mono-exponential function, the temperature T of a pixel (i, j) at a time t was given as:

$$T(i,j,t) - T(i,j,0) = [T(i,j,\infty) - T(i,j,0)] \times [1 - \exp(-\mu t)], \qquad (5.1)$$

where the constant μ depends on the blood perfusion underneath the skin surface as well as the thermal conductivity of the tissue. The μ-value thermal imaging system provided a colour-coded 250×230 image of μ values of each pixel calculated from sequential thermograms. Despite the observation of Steketee and Van Der Hoek [22] that it is necessary to discard the initial part of the transient if a mono-exponential thermal recovery is to be useful, it was thought that µ-thermograms could reveal information about pathophysiological abnormality.

The effectiveness of the μ-value thermal imaging system was initially assessed for a patient with a proven cancer in the right breast and a false negative steady state thermogram performed after 20 min acclimation in a room temperature of 21 °C. After 2 min chilling by using cold air moved over the breast surface using an electric fan, the temperatures of the right and left nipples were recorded every 15 s during rewarming. Measurements were taken over a period of approximately 4 min. Thermal recovery curves showed that the temperature of the left nipple was lower than the temperature of the right one. Furthermore, the computer system processed a sequence of 6 thermograms taken every 15 s by subtracting the temperature values in each thermogram from corresponding values in the previous one in order to produce a colour-coded μ-value image.

Two years Later, Uchida et al. [33] used the μ-value thermal image processing system to analyse 18 patients with breast cancer which had been incorrectly diagnosed by steady state thermography and dynamic thermography (sequential and subtraction). Steady state thermograms were taken in a room temperature of 23 °C after 10 min acclimation. Then thermograms were taken sequentially at intervals of 15 s, following exposure to cold air applied using an electric fan for a period of 2 min. The diagnosis criteria used for breast thermography at steady state and after cooling depended on qualitative and quantitative findings of:

1. Asymmetric hot spot on the steady state thermogram
2. Asymmetric abnormal exaggeration of vascular pattern
3. Significant differences in the thermal map
4. Positive heat patterns in thermograms taken sequentially
5. A hot spot in the subtracted thermogram

The presence of sign 1 or sign 2 was considered positive in terms of diagnosis using steady state thermography. However, several problems including patient movement as well as breathing have limited the diagnostic value of µ-thermography which corrected 4 cases among 12 false negative thermograms and 4 cases among 6 false positive thermograms. The authors also pointed out thermal artefacts caused by uneven air flow distribution over the curved surface of the breast and suggested that better results could be produced using different cooling methods. The accuracy of µ-thermography was then reassessed after incorporating motion compensation analytical tools by examining 26 patients with non-palpable breast cancer [34].

A correct diagnosis was obtained in 55% cases using steady state thermography, 14% using dynamic thermography (sequential and subtraction) and 11% using μ-thermography.

Later, Ohashi and Uchida [35] reviewed the effectiveness of steady state and subtraction thermography in the diagnosis of 728 patients with proven breast cancer and 100 patients with benign breast diseases between 1989 and 1994. However, for patients with breast cancer, the diagnostic accuracy improved from 54% when steady state thermography was used to the much larger value of 82% in the case of dynamic thermography after cold stress, without any associated increase in the rate of false positives. For cases of benign breast diseases, the overall false positive rate of steady state thermography was 41% versus 29% using subtraction thermography. Although Ohashi and Uchida emphasised the merit of μ-thermography as a future diagnosis tool, the current authors are not aware of any further work that has been published since 1997.

More recently, Arora et al. [36] conducted a 2-year study to evaluate an advanced digital thermography system for cancer detection. The study involved 92 women whose average age was 51 years, the range being between 23 and 85, all of whom had a suspicious breast lesion which had been identified using mammography or ultrasound. Prior to thermography examination, the group of patients underwent biopsy in a prospective double-blind trial. 60 out of 94 biopsies suggested the presence of a malignancy and 34 suggested no malignancy. The majority of malignancies were infiltrating ductal carcinoma and the invasive tumours ranged in size from 0.5 to 14 cm. The clinical study used the Sentinel BreastScan, an advanced digital thermography system manufactured by Infrared Science Corporation comprising a digital camera with a sensitivity of 0.08 °C and a spatial resolution of 320×240 pixels. Unlike other infrared system, the Sentinel BreastScan is a fully automated diagnostic tool that employs artificial intelligence to provide a fully interpreted real-time test report to the doctor. During the thermography procedure, a series of more than 100 thermograms were collected while cool air was directed at the breasts for approximately 4 min. Specific thermal parameters for each breast were extracted and compared using asymmetry analysis during post-processing of thermograms recorded during cooling. The software then produced colour-coded images of the breast indicating suspicious areas as well as all measured thermal breast parameters. Dynamic thermography identified 58 of 60 malignancies; the sensitivity was 97% and the specificity 44%.

6 Active Dynamic Breast Thermography

Active Dynamic Thermography (ADT) refers to dynamic thermography in non-destructive evaluation of materials [37]. It is based on retrieving thermal parameters of a tested object from its surface thermal response to an active external excitation which involves heating or cooling. A series of thermal images are

processed for the calculation of parametric images mainly thermal constant profiles that are strongly correlated with the presence of defect in the tested object.

Advanced infrared imaging systems and image processing tools are being developed to retrieve information from thermal recovery response after removing the external excitation [38–40]. By assuming a Fourier heat conduction model in tissue, two-exponential models have been used to fit temperature transients at the surface of the tissue during thermal recovery after heating or cooling:

$$T_c(x, y, t) = T_e + \Delta T_1 \exp(-t/\tau_{1c}(x, y)) + \Delta T_2 \exp(-t/\tau_{2c}(x, y)) \qquad (6.1)$$

$$\begin{aligned} T_h(x, y, t) = T_e &+ \Delta T_1(x, y).[1 - \exp(-t/\tau_{1h}(x, y))] \\ &+ \Delta T_2(x, y).[1 - \exp(-t/\tau_{2h}(x, y))] \end{aligned} \qquad (6.2)$$

where T is the temperature transient during thermal recovery from heating or cooling, T_e is the temperature at steady state, τ_1 and τ_2 time constants, the subscripts c and h indicates cooling and heating phase, respectively. Time constants τ_1 and τ_2 of the models can be identified using readily available nonlinear fitting functions. In order to establish diagnosis criteria, averaged values for time constants of the healthy tissue, $\bar{\tau}_{ref}$, are used as references in normalised time constants defined by:

$$\tau_{norm} = \frac{\tau - \bar{\tau}_{ref}}{\tau + \bar{\tau}_{ref}} \qquad (6.3)$$

Normalised values of time constant would eliminate any change in blood perfusion in a patient or between a group of patients [39].

Different types of excitations and cooling mode have been used. Forced convection was applied using two different cooling units. The first is a cryotherapeutic unit designed for clinical applications that uses expanded carbon dioxide mixed with air and provides a cooling stream from 0 °C to ambient temperature. The second industrial air conditioning unit blows air at temperatures in the range of 5 °C to ambient temperature. Both units are supplied with disposable air filters to insure aseptic conditions during cooling. Ice held in a thin plastic bag was used for localised cooling of the tested tissue. Controlled cooling periods were between 30 and 60 s. Halogen lamps were used to heat the surface of tissues to a maximum temperature of 48 °C.

Active Dynamic Thermography procedures have been applied for burns diagnosis [41], quality evaluation of cardio-surgery procedures [42] and post-surgery wound healing [43]. Despite the promising results that have been obtained [38], the use of ADT in breast diagnosis has received little attention [44, 45]. Active dynamic thermography was performed on a small-scale study group of three women with proven breast cancer (mammography and biopsy). In order to achieve heating, the breast surface was exposed to light from halogen lamps of electrical power of 1000 W located 50 cm from the breast surface, for a period of 30 s. Parametric images of time constants τ_{1c} and τ_{2c} were obtained but not presented for all the

three women's breasts. Further, interpretations of parametric images were not given because of the complex structure of breast tissue, limited heating power and limited depth of detectable cancers.

Generally, research studies have identified problems of implementing ADT in medicine caused by the complex structure of tissues, variability of thermal properties between patients, movement of patient during imaging due to breathing and technical limitations inherent to the type of external heating or cooling source. Therefore, the main challenges of the research studies were as follows [46]:

1. Define optimal excitation sources which induce the best thermal contrast in each specific medical diagnosis problem. Sources should be non-invasive, safe and aseptic, easy to use and reliable.
2. Determine the required characteristics of the imaging system (thermal resolution and spectral range) to be used with a particular excitation.
3. Identify sources of errors that may affect the final parametric images.

The performances of heating and cooling sources have been extensively investigated for medical applications. Cooling was found to be safer than heating [46]. The change of skin temperature up to 20 °C was found comfortable for a patient. The signal to noise ratio was higher for cooling than for heating. It was also suggested that heating should never exceed 42 °C and that the best condition for cooling is at room temperature to avoid thermal gradient and heat exchange with the environment. However, when electric fans were used for cooling, it was difficult to control the energy level and the uniformity of cooling. The later also depends on the shape of the tested tissue. Overall, cooling experiments showed that the excitation should not last for more than one minute in order to minimise the effect of the thermoregulatory mechanism. For the instrumentation requirement, a minimum infrared camera resolution of 0.1 °C and a recording rate of at least 30 images per second was recommended. Interference between the heating sources and the thermal radiation from the tested tissue should be avoided. To improve the quality of parametric images, thermal images should be pre-processed using algorithms for motion compensation caused by unintentional patient displacement and for noise filtering. In some applications of ADT, recording of thermal images have to be synchronised with natural movement of the body caused mainly by breathing or by heart beating in the case of cardiovascular surgery.

However, it has been reported that the main challenge to which are faced every application of ADT in medicine, is the interpretation of the parametric images of time constants. It has been observed that different stresses yield different parametric images reflecting information about blood perfusion, thermal diffusivity and metabolic heat generation. Nevertheless, promising clinical results were obtained by a versatile instrumentation that could be used for the quantitative and qualitative analysis of dynamic thermography in various medical applications [38].

7   Numerical Modelling of Breast Dynamic Thermography

Numerical simulations are a powerful means of understanding and optimising breast thermography. So far, several numerical techniques have been used to examine conditions that affect breast surface temperature and steady state thermal contrast in the presence of a tumour. The effect of factors such as blood perfusion, tumour characteristics including depth and diameter as well as environmental characteristics affecting thermography measurements, namely ambient temperature and heat transfer coefficient, have all been investigated [47–53]. Nevertheless, none of these numerical methods obtained the details of tumour characteristics from steady state and transient thermograms.

In the late 70s, Chen et al. [54] studied the feasibility of determining interior information from temperature transients, and investigated its limitations. It was shown that it is almost impossible to determine the metabolic heat of an embedded source from sequential thermograms. However, Chen et al. [54] proposed a theoretical method to determine blood perfusion of a volumetric heat source from time-dependent thermographic observations. A two-dimensional numerical model was used with no specific inversion technique. The procedure consists of varying the air flow and the ambient temperature impulsively and recording the temperature transients for a fixed duration. Computer-based harmonic analysis was then used to determine the blood perfusion.

Although it is useful to detect the presence of a tumour by determining the change in blood perfusion in the surrounding tissue after cooling, it is also interesting to use thermal recovery to derive information about tumour's parameters such as depth, diameter and blood perfusion. Such characterisation represents numerically an ill-posed inverse numerical problem that can be impractical to solve due to the complexity of the boundary conditions. Therefore, the main objectives of numerical modelling of breast dynamic thermography are to examine optimal conditions for cooling that induce larger thermal contrasts during thermal recovery of the breast and to identify thermal recovery parameters that could be correlated with tumour's characteristics.

To this end, it is necessary to describe a heat transfer model for the breast with and without a tumour and to implement a numerical scheme for a breast's model geometry. This later should provide a steady state solution for breast thermography and transient solutions during cooling and the subsequent thermal recovery.

7.1   A Heat Transfer Model for the Breast

Heat conduction, blood perfusion and metabolic heat generation all influence the mechanism of heat and associated temperature fields in biological materials. There is a general agreement that it is difficult to model the mechanism of blood perfusion, due to the complex structure of the perfused tissue. There have been two types of

approaches: a continuum approach and a vascular approach. In the continuum approach [23, 55–57], a single parameter is used to represent the effect of all blood vessels. On the other hand, in the vascular approach each blood vessel is considered individually in terms of its thermal effect [58, 59]. The earliest continuum model, Pennes [23] bioheat transfer equation, represents the effects of the blood flow using a single heat source, which is nonlinear in the sense that it is itself temperature dependent. Other models have been proposed to overcome the shortcomings of Pennes model by considering the influence on heat transfer of blood flow within elements of the vascular network. There are several critical reviews of heat transfer models in biological materials, including [60–64]. However, Pennes equation has been shown to have a high level of validity when vessels larger than 500 μm are concerned [65].

Because the use of a vascular model requires detailed knowledge of the breasts microvascular network which varies from one woman to another, continuum models are more attractive, and Pennes bioheat equation (7.1) has been extensively used to model heat transfer in the breast. We recall this as:

$$\rho c \frac{\partial T}{\partial t} = \nabla.k\nabla T - \omega_\mathrm{b}\rho_\mathrm{b}c_\mathrm{b}(T - T_\mathrm{a}) + Q_\mathrm{m}, \tag{7.1}$$

where the symbols have the meanings given previously. Heat transfer between the surface of the breast and the surrounding ambient is by radiation and convection, with additional cooling as the result of evaporation of sweat. These processes can be expressed as [66]:

$$-k\frac{\partial T}{\partial n}\bigg|_{\mathrm{skin}} = h_\mathrm{f}(T_\mathrm{s} - T_\mathrm{f}) + \sigma\varepsilon\big(T_\mathrm{s}^4 - T_\mathrm{f}^4\big) + Q_\mathrm{e}, \tag{7.2}$$

where n is the normal vector at the surface; h_f (W m^{-2} C^{-1}) is the convection heat transfer coefficient; T_s and T_f are temperature of the skin and the surrounding air, respectively; ε is the skin emissivity, and σ the Stefan–Boltzman constant; Q_e is the evaporative heat loss.

Since changes in air temperature, circulation and humidity all cause changes in the thermogram of a breast, a strict protocol is needed for recording thermograms. Protocols developed so far include environmental specification, as well as requirements relating to the patient's condition. Imaging room temperature should fall within the range 18–22 °C to promote cooling by vasoconstriction and the flow of heat to the breast surface by air convection needs to be minimized [66]. To this end, heat-generating equipment such as computers should be located outside the examination room. Amalu et al. [67] pointed out that such temperatures do not cause patients to either shiver or perspire. Patients are also ideally recommended to avoid consuming alcohol, tea or coffee, eating heavy meals, smoking, sunbathing, using cosmetic preparations or undertaking strenuous exercise before examination, since these can have an effect on skin temperatures [68, 69].

When appropriate protocols are followed, Draper and Boag [66] showed that total heat loss may be considered to be proportional to $(T_s - T_f)$, assuming that $(T_s - T_f)$ is small. Thus the boundary condition at the breast surface is reduced to

$$-k\frac{\partial T}{\partial n}\bigg|_{skin} = h_0(T_s - T_f), \tag{7.3}$$

where h_0 is a constant referred to as the surface conductance which combines the effect of radiative and convective heat coefficients:

$$h_0 = h_{conv} + h_{rad} \tag{7.4}$$

If the environment is suitably controlled, the heat loss associated with evaporation may be rendered negligible. It is difficult to estimate accurately the convection heat loss from the patient. However, Winslow et al. [70] studied the influence of air movement on convective heat loss from the whole body. For wind speeds between 2.6 and 0.46 m s^{-1} they derived the empirical formula:

$$h_{conv} = 12.1\left(v^{0.5}\right) \text{W m}^{-2}\,^{\circ}\text{C}^{-1}, \tag{7.5}$$

where v is the wind speed. This approach yields values of h_{conv} for the upper breast surface of 4.6 W m^{-2} $^{\circ}$C^{-1}and for the lower surface of the breast of 5 W m^{-2} $^{\circ}$C^{-1}. If $(T_s - T_f)$ is small in comparison to the average temperature T_m, then we can consider the heat loss due to radiation to be $4\sigma\varepsilon T_m^3$ where $T_m = (T_s + T_f)/2$, so that

$$h_{rad} = 4\sigma\varepsilon T_m^3 \tag{7.6}$$

Mitchell et al. [71] found that, at thermal radiation wavelengths, the emissivities of black and white skin were within 1% of unity throughout the whole range. Since T_m is likely to vary between a minimum of 22 °C and a maximum of 27 °C, Eq. (7.6) suggests that h_{rad} varies between 5.95 and 6.15 W m^{-2} C^{-1}.

Draper and Boag [66] recorded a total heat loss of $h_0 = 10.4$ W m^{-2} C^{-1} when ambient air is stationary and values in the range of $h_0 = 12$ and 24 W m^{-2} C^{-1} when air at speeds in the range of 0.2–2 m s^{-1} flows over the surface of the breast. Osman and Afify [72], on the other hand, evaluated the heat transfer coefficient representing the combined effect of radiation, convection and evaporation, as $h_0 = 13.5$ W m^{-2} C^{-1}.

The presence of a tumour in the breast can be accounted for by implementing the corresponding metabolic heat generation and blood perfusion or thermal conductivity. Gautherie et al. [73] showed that the time necessary for the tumour to double, τ, and the metabolic heat are related by a hyperbolic function:

$$Q_m = \frac{3.27 \times 10^6}{468.5\ln(100D) + 50} \text{W m}^{-3}, \tag{7.7}$$

where D is the diameter of the tumour assumed of spherical shape. Gautherie [74] estimated a global effective thermal conductivity for a cancerous breast tissue, the value of which was enhanced to include the effect of blood perfusion. The estimated value was 0.511 W m^{-1} °C^{-1}. By assuming that the thermal conductivity of the tumour tissue matches that of the glandular tissue at 0.48 W m^{-1} °C^{-1}, Ng and Sudharsan [51] used the enhancement in the thermal conductivity value of 0.03 W m^{-1} °C^{-1} to calculate tumour blood perfusion. Using mathematical and physical models, Priebe [75] established an incremental relationship between blood flow and thermal conductivity: a variation of blood flow of 150 ml min^{-1} per 100 g of tissue results in a change of thermal conductivity of about 0.05 W m^{-1} °C^{-1}. Correspondingly, the enhancement in the tumour blood perfusion is 90 ml min^{-1} per 100 g.

7.2 A Numerical Procedure for Transient Thermography

To solve the previous heat transfer model, a breast's model geometry needs to be defined. From a knowledge of breast anatomy [76, 53] developed a two dimensional model in which the various layers of the breast (subcutaneous, gland and fat), were modelled using layers of various thickness close to the actual shape. Later, a three dimensional breast model with an embedded tumour was used to examine numerically the effectiveness of subtraction thermography during breast thermal recovery after cold stress [77]. The cooling of the breast was not considered, although a lumped thermal analysis was used to estimate the extent to which the cold layer, induced by an instantaneous change in the ambient temperature, penetrated the breast and to develop an approximate model for vasoconstriction. During thermal recovery, a time-dependent model for blood perfusion was used for the three quadrants of the breast affected by vasoconstriction whilst the tumour of diameter 32 mm, was located at the upper quadrant of the breast that was assumed unaffected by cold stress. The model was numerically solved using FASTFLO calculator, which solves partial differential equations dedicated for CFD (computational fluid dynamics). The temperature's map observed after 60 min of recovery from cold stress was almost the same as the steady state temperature distribution. Unlike the observation of Usuki et al. [31] that subtraction thermography may enhance thermal contrast, subtraction of thermal profiles obtained for 1, 3 and 5 min during thermal recovery did not yield any improvement in the thermal contrast or give information not available using the steady state thermogram.

Numerical simulation of dynamic thermography using a three-dimensional model based on a hemisphere with and without a tumour could pose problems in terms of computer processing times and memory storage due to the large number of thermograms that would need to be captured and processed during the phase of thermal recovery. In addition, the use of such models for comparing the effectiveness of different cooling methods is rather impractical. An alternative breast

model geometry has been suggested by Amri et al. [47]. Based on the model of Ng and Sudharsan [51], the breast model shown in Fig. 3 consists of a 5 mm thick fat and gland which thickness H of at least 45 mm. The embedded tumour was assumed to be spherical and of diameter D and metabolic heat Q_m. The use of such a model for steady state thermography has shown consistency with the results obtained using hemispherical models. The breast model of Fig. 3 was recently used by Amri et al. [78] to examine numerically the dynamic breast thermography after cold stress using the Transmission Line Matrix (TLM) method [79].

The numerical procedure starts by solving Pennes bioheat equation (7.1) at steady state, subject to the following conditions:

$$-k\frac{\partial T}{\partial z} = h_0(T_f - T) \quad \text{at } z = 0 \text{ and } T = T_c \text{ at } z = H \tag{7.8}$$

$$-k\frac{\partial T}{\partial x} = 0 \quad \text{at } x = 0 \text{ and } -k\frac{\partial T}{\partial x} = 0 \text{ at } x = L \tag{7.9}$$
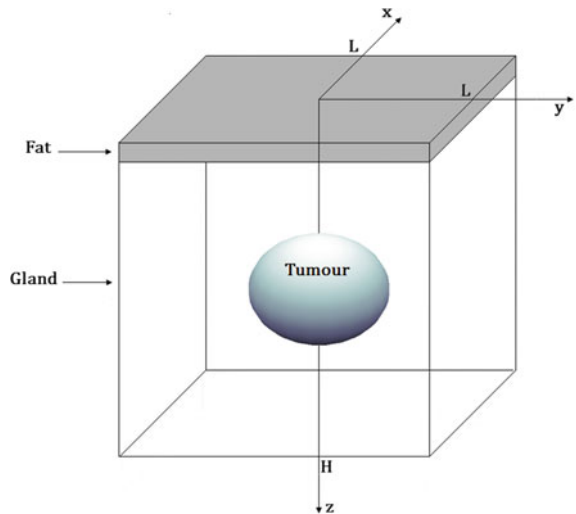
$$-k\frac{\partial T}{\partial y} = 0 \quad \text{at } y = 0 \text{ and } -k\frac{\partial T}{\partial y} = 0 \text{ at } y = L \tag{7.10}$$

Perfect thermal contact is assumed between the breast tissue and the tumour.

$$\begin{cases} T_b(x,y,z) = T_t(x,y,z) \\ \frac{\partial T_b}{\partial n} = \frac{\partial T_t}{\partial n} \end{cases} \tag{7.11}$$

Subscribes b and t denote breast and tumour respectively. The change in the temperature of the surface, associated with the presence of a tumour, is evaluated

Fig. 3 A three-dimensional breast model geometry [78]

using a parameter known as the steady state thermal contrast, C_{ss}. This is defined as the difference between the maximum temperature reached in the presence of a tumour and the temperature at the surface of the normal breast.

$$C_{ss} = \max(T_{tumour}) - T_{healthy} \tag{7.12}$$

Tumour diameters of 10, 20 and 30 mm at depths of dp = 5, 7.5, 10, 15, 20 and 30 mm were considered. The depth is defined as the distance between the breast surface and the top of the tumour. The steady state thermal contrast C_{ss} illustrated in Fig. 4 shows that, irrespective of tumour diameter, steady state thermography is best suited to detect tumours at depths less than 20 mm. An infrared camera with a thermal resolution of 0.1 °C can be used, though higher resolution is desirable. Beyond this depth, it is difficult to distinguish the tumour diameter and depth as they lead to almost identical steady state thermal contrast C_{ss}. Thus, if the thermal contrast is small, this may indicate a deep tumour but does not give information about the tumour's diameter.

With the tissue initially in a state of thermal equilibrium, a cold stress temperature T_{cold} was applied on the surfaces of both the normal (healthy) breast and the cancerous breast during a cooling period t_{cool}. Pennes equation was then solved using a constant boundary condition:

$$T = T_{cold} \quad \text{for} \quad 0 < t \leq t_{cool} \tag{7.13}$$

To estimate how far into the breast tissue the effect of surface chilling penetrates, it is helpful to define the thermal penetration depth δ_p. The temperature of the tissue when the penetration depth has been reached should satisfy [24]:

$$\frac{\partial T(z,t)}{\partial z} = 0 \quad \text{at} \quad z = \delta_p(t) \tag{7.14}$$

Fig. 4 Thermal contrast plotted against tumour diameter and depth at steady state
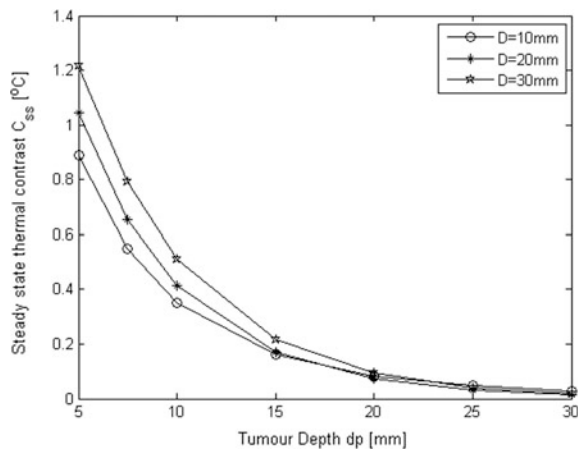
$$T(z,t) = T_i \quad \text{at} \quad z = \delta_p(t) \tag{7.15}$$

where T_i is the initial temperature. Although some clinical studies that have been reported in earlier sections used fan cooling of the breast, it has been criticised for producing nonuniform cooling and for being difficult to control. Therefore localised cooling seems to be an ideal choice as long as cooling is applied for short periods of time to avoid patient's shivering.

In order to study the effect of cold stress temperature T_{cold} and the cooling period t_{cool} on the thermal transients, cold temperatures of 5, 10 and 15 °C and cooling periods of 10, 20, 30, 60 and 120 s have been examined. Figure 5 represents the variation of the penetration depth versus the cooling time. The horizontal line represents the rear boundary of the fat layer. Equations (7.14) and (7.15) predict that a minimum cooling period of 20 s is required for the cold front to reach the gland region where a tumour is likely to be. When cooling for a maximum of 2 min, the thermal cold front penetrates about 14 mm into the breast, so that tumours located deeper in the breast are uncooled.

After the cold stress was removed, the surface temperatures on both breasts were recorded throughout the rewarming period of 60 min; this is consistent with [23] that skin temperature at the forearm needs 30–60 min to return to steady state after the end of chilling. During thermal recovery, both normal and cancerous breasts exchange with adiabatic ambient via radiation and convection. To evaluate the efficiency of the cold stress on the enhancement of temperature differences between the breasts, the transient thermal contrast is again defined by:

$$C_{max}(t) = \max[T_{tumour}(t)] - T_{healthy}(t) \tag{7.16}$$

To enable tracking of the maximum temperature, the steady state thermogram may help since the location of the maximum temperature can be identified. It might then be helpful to mark the hot spot location on the cancerous breast and on the

Fig. 5 Influence of cooling period on the thermal penetration depth. The *horizontal line* indicates the edge of the fat layer
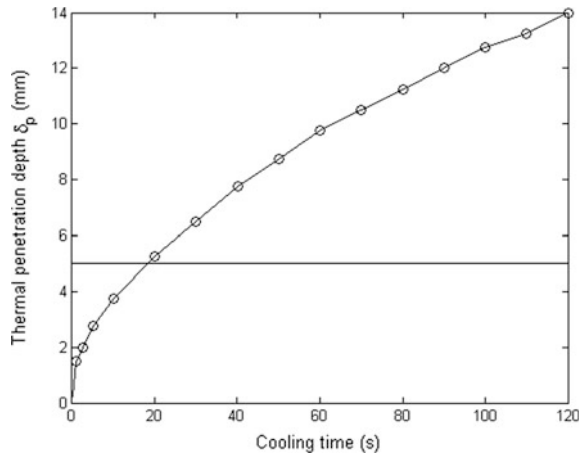
corresponding contralateral symmetrical part of the normal breast. There is then no need to monitor the dynamic change in the surface temperature of the whole of the suspicious breast so storage of enormous amounts of data can be avoided.

The diagnostic value of cold stress was assessed by comparing the transient and steady state thermal contrasts and by extracting information about the tumour's size and depth. The effects of the temperature and the duration of the chilling process on the transients were examined for different tumours at different depths and of different diameters.

Figure 6 illustrates a typical transient thermal contrast during the rewarming transient. Since the objective of dynamic thermography is to enhance thermal contrast, it is useful to use the steady state thermal contrast as a reference. This is identified by the dash dotted line in Fig. 6. Initially, the contrast rises to the steady state thermal contrast C_{ss}, then increases further as time continues to reach a contrast peak, C_{peak}, at a peak time τ_{peak}. After this time, the thermal contrast decreases and thermal equilibrium is reached by the end of the monitored period.

To evaluate how useful dynamic thermography after cold stress can be, the magnitude of the contrast peak and its corresponding peak time, have been derived from thermal contrasts transients. This has been done for tumours having a range of diameters and being located at a range of depth. The data obtained are presented in Fig. 7.

Figure 7a shows similar trends as steady state thermal contrast shown in Fig. 4. It seems that the magnitude of the contrast peak is determined by the penetration depth of figure (Fig. 5). Higher contrast peak values have been obtained for tumours which have been affected by cooling located at depth less than 15 mm. Dynamic thermography was unable to enhance thermal contrast for tumours at depth 20 mm or more. It has also found that the use of lower temperatures does increase the transient peak for tumours located near the surface. This suggests that, chilling temperatures marginally less than ambient temperature are all that is necessary and chill duration needs to be no longer than 1 min. Such a protocol should not prove particularly uncomfortable or inconvenient to patients.

Fig. 6 Schematic of the variation of the maximum contrast as thermal recovery occurs after the end of cold stress. The *dashdot horizontal line* represents the steady state thermal contrast, and the *filled circle* corresponds to the contrast peak
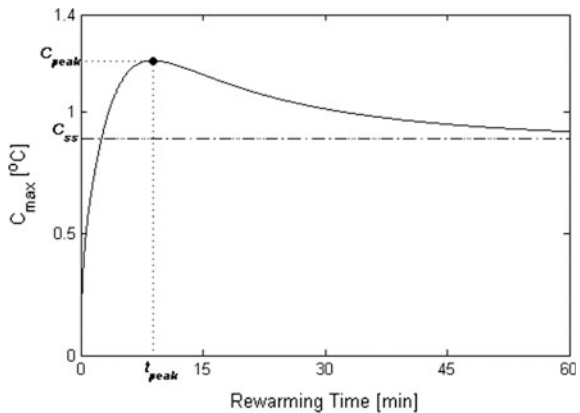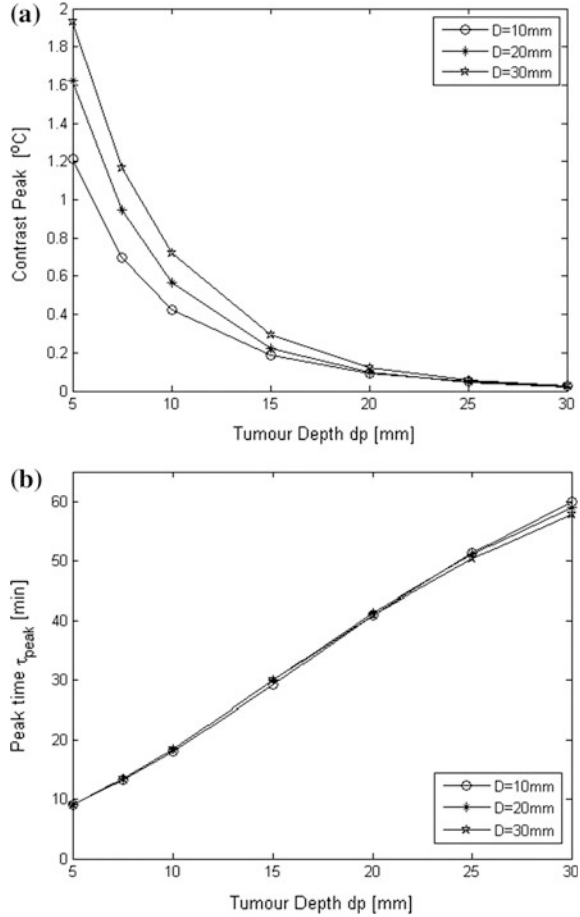
Fig. 7 Effect of tumour size and depth on **a** the contrast peak and **b** the corresponding peak time after cooling at $T_{cold} = 5\ °C$ during $t_{cool} = 1$ min

The measure of the corresponding peak time values shown in Fig. 7b would be critically dependent on the responsivity associated with the infrared camera in order to locate the contrast peak. This is particularly important for tumours located 20 mm deep and more. Nevertheless, the peak time seems to be directly related to the tumour's depth and independent of the tumour's diameters. It was also found that the peak time does not vary significantly with the magnitude of the cooling temperature or the period of cooling. This would make details of the measurement protocols in the clinical environment less important. In the light of the continuing progress in the infrared imaging technology and the development of software that include motion as well as noise compensation tools, measurements of the peak time may become more feasible in the near future.

8 Conclusion

Dynamic thermography techniques have been utilised in a variety of diagnostic applications including breast cancer. Clinical experiments have observed enhanced thermal contrast after artificially cooling the breast and have demonstrated the ability of increasing the accuracy of breast cancer diagnosis. Various computer techniques have been deployed to process sequential thermograms during thermal recovery of the breast including subtraction thermography and μ-thermography. These techniques have been applied to small-sample breast cancer studies and have revealed information pertaining to the change in thermal parameters of the breast associated with the presence of a tumour. The complexity of the thermal findings has caused major difficulties for the clinical interpretation of thermal parametric images. Some research studies investigated the change in blood perfusion caused by the presence of a tumour. These studies employed localised cooling on the area that shows hot spot on steady state thermograms and its contralateral part. Although results were promising, the rate of false positive was a major constraint to this technique and might relate to protocol and instrumentation issues. Other clinical studies used the autonomic cold challenge by cooling patient's extremities in order to identify new tumour's blood vessels known as neoangiogenesis but research findings did not correlate with the presence of the tumour.

In an attempt to understand skin's temperature transient after cold stress, a mathematical model for a homogenous one-dimensional skin slab was developed. The analytical solution showed that a two-exponential temperature transient model is a good fit for the thermal recovery of the skin after direct chilling and that the corresponding time constants are related to the thermal properties of the tissue as well as to its blood perfusion. When modelling skin with an embedded heat source representing a tumour, a numerical study showed that it is possible to extract a tumour's blood perfusion from temperature transients after cooling the skin by convection. However, it was not possible to extract the tumour's parameters such as metabolic heat, size and location during thermal recovery and that even the use of inverse numerical models would fail, due to the complexity of the problem. However, a more recent simulation study of dynamic breast thermography after cooling the breasts at a constant temperature for a period of time of two minutes or less, showed an enhancement in the contrast peak for tumours at depth 20 mm or less. Furthermore, it was found that the time corresponding to the contrast peak, referred to as the peak time, was directly related to the tumour's depth and independent of the tumour diameter. It was also shown that the peak time does not correlate with the cold stress temperature or the duration of the cooling phase which give it the potential to be an indicator of tumour depth. Although it might be interesting to obtain information about the tumour's diameter, depth is the more important parameter in breast tumours diagnosis as the tumour's diameter can be estimated by palpation during physical examination.

Until now, different techniques have been applied to cool the breast and to process the thermal recovery. Overall, each processing technique of breast thermal

recovery has contribute unique information about the presence of an abnormality in the breast such as a change in blood perfusion, an alteration in the breast thermal parameters or by estimating its depth. Therefore, in the light of the continuing progress in infrared imaging instrumentation, dynamic breast thermography justifies thorough research interest in order to conclude about its usefulness in breast cancer diagnosis.

References

1. Lawson, R.: Implications of surface temperatures in the diagnosis of breast cancer. Can. Med. Assoc. J. **75**, 309 (1956)
2. Williams, K.L., Williams, F.L., Handley, R.: Infra-red radiation thermometry in clinical practice. Lancet **276**, 958–959 (1960)
3. Williams, K.L., Williams, F.L., Handley, R.: Infra-red thermometry in the diagnosis of breast disease. Lancet **278**, 1378–1381 (1961)
4. Barnes, R., Gershon-Cohen, J.J.: Clinical thermography. JAMA **185**, 949–952 (1963)
5. Barnes, R.B.: Thermography of the human body. Science (Infrared-radiant energy provides new concepts and instrumentation for medical diagnosis) **140**, 870–877 (1963)
6. Freeman, H., Linder, F.E., Nickerson, R.F.: The bilateral symmetry of skin temperature: one figure. J. Nutr. **13**, 39–49 (1937)
7. Sheard, C., Williams, M.M.D.: Skin temperatures of the extremities and basal metabolic rates in individuals having normal circulation. Proc. Staff Meet. Mayo Clin. **15**, 758–762 (1940)
8. Williams, K.L.: Infrared thermometry as a tool in medical research. Ann. N. Y. Acad. Sci. **121**, 99–112 (1964)
9. Williams, K.L.: Pictorial heat scanning. Phys. Med. Biol. **9**, 433 (1964)
10. Barnes, R.B.: Thermography. Ann. N. Y. Acad. Sci. **121**, 34–48 (1964)
11. Astheimer, R.W., Wormser, E.M.: High-speed infrared radiometers. J. Opt. Soc. Am. **49**, 179–183 (1959)
12. Amalric, D., Giraud, D., Altschule, C., Spitalier, J.: Value and interest of dynamic telethermography in detection of breast cancer. Acta Thermograph **1**, 89–96 (1976)
13. Gautherie, M., Haehnel, P., Walter, J., Keith, L.: Long-term assessment of breast cancer risk by liquid-crystal thermal imaging. Prog. Clin. Biol. Res. **107**, 279–301 (1981)
14. Cockburn, W.: Announcement of Official Change in Thermal Reporting [Online]. Available: http://www.thermologyonline.org/breast/breast_q_a/bqa_coldstress.htm (2005)
15. Kane, R.L.: Considerations in the Applications of Various Cooling Methods During Breast Thermography Stress Studies [Online]. International Academy of Clinical Thermology. Available: http://www.iact-org.org/articles/articles-considerations.html (2002)
16. Leando, P.: Cold Stressing Breasts and Why Don't We Do It Anymore and the Thermal Rating System [Online]. American College of Clinical Thermology. Available: http://acct-blog.com/category/cold-stressing-breast/ (2003)
17. Amalu, W.C.: Nondestructive testing of the human breast: the validity of dynamic stress testing in medical infrared breast imaging. In: Engineering in Medicine and Biology Society, 2004. IEMBS'04. 26th Annual International Conference of the IEEE, pp. 1174–1177. IEEE (2004)
18. Nagasawa, A., Okada, H.: Thermal recovery. In: Atsumi, K. (ed.) Medical Thermography. University of Tokyo Press, Tokyo (1973)
19. Cary, J., Mikic, B.: A thermal analysis of human tissue with applications to thermography. In: 2nd International Symposium on the Detection and Prevention of Cancer, Bologna, Italy (1973)

20. Cary, J., Kalisher, L., Sadowsky, N., Mikic, B.: Thermal evaluation of breast disease using local cooling 1. Radiology **115**, 73–77 (1975)
21. Steketee, J.: Thermografie van het voorhoofd. *Jubilee edition of reports*. Erasmus University, Rotterdam (1978)
22. Steketee, J., Van der Hoek, M.: Thermal recovery of the skin after cooling. Phys. Med. Biol. **24**, 583 (1979)
23. Pennes, H.H.: Analysis of tissue and arterial blood temperatures in the resting human forearm. J. Appl. Physiol. **1**, 93–122 (1948)
24. Carslaw, H.S., Jaeger, J.C.: Conduction of Heat in Solids, 2nd edn. Clarendon Press, Oxford (1959)
25. Spiegel, M.: Schaum's Outline of Laplace Transforms. McGraw-Hill Education (1965)
26. Newman, P., Evans, A.L., Davison, M., Jackson, I., James, W.B.: A system for the automated diagnosis of abnormality in breast thermograms. Br. J. Radiol. **50**, 231–232 (1977)
27. Uchida, I., Onai, Y., Ohashi, Y., Tomaru, T., Irifune, T.: quantitative diagnosis of breast thermograms by a computer. J. Jpn Radiol. Soc. Radiol. **39**, 401–411 (1979)
28. Winter, J., Stein, M.A.: Computer image processing techniques for automated breast thermogram interpretation. Comput. Biomed. Res. **6**, 522–529 (1973)
29. Ziskln, M.C., Negin, M., Piner, C., Lapayowker, M.S.: Computer diagnosis of breast thermograms. Radiology **115**, 341–347 (1975)
30. Geser, H., Bosinger, P., Stucki, D., Landolt, C.: Computer-assisted dynamic breast thermography. Thermology **2**, 538–544 (1987)
31. Usuki, H., Teramoto, S., Komatsubara, S., Hirai, S., Misumi, T., Murakami, M., Onoda, Y., Kawashima, K., Kino, K., Yamashita, K.: Advantages of subtraction thermography in the diagnosis of breast disease. Biomed. Thermol. **11**, 286–291 (1991)
32. Uchida, I., Ohashi, Y., Onai, Y., Yamada, Y., Tomaru, T.: Quantitative analysis of sequential thermograms 1. In: Development of a Physiological Functional Image Processing System for Dynamic Thermography after Cooling (1988)
33. Uchida, I., Ohashi, Y., Sato, Y., Yamada, Y., Oyamada, H., Tomaru, T., Onai, Y., Ito, A.: Effectiveness of pathophysiological functional thermal images in the diagnosis of breast thermography. Jpn Radiol. Phys. **10**, 101–106 (1990)
34. Ohashi, Y., Uchida, I.: Some considerations on the diagnosis of breast cancer by thermography in patients with nonpalpable breast cancer. In: Engineering in Medicine and Biology Society, 1997. Proceedings of the 19th Annual International Conference of the IEEE, vol. 2, pp. 670–672, 30 Oct–2 Nov 1997
35. Ohashi, Y., Uchida, L.: Applying dynamic thermography in the diagnosis of breast cancer. Eng. Med. Biol. Mag. IEEE **19**, 42–51 (2000)
36. Arora, N., Martins, D., Ruggerio, D., Tousimis, E., Swistel, A.J., Osborne, M.P., Simmons, R.M.: Effectiveness of a noninvasive digital infrared thermal imaging system in the detection of breast cancer. Am. J. Surg. **196**, 523–526 (2008)
37. Maldague, X.P.: Theory and Practice of Infrared Technology for Nondestructive Testing. Wiley, New York (2001)
38. Kaczmarek, M., Nowakowski, A.: Active IR-thermal imaging in medicine. J. Nondestr. Eval. **35**, 1–16 (2016)
39. Nowakowski, A., Kaczmarek, M.: Active dynamic thermography—problems of implementation in medical diagnostics. Quant. InfraRed Thermogr. J. **8**, 89–106 (2011)
40. NowakowskI, A.: Quantitative Active Dynamic Thermal IR-Imaging and Thermal Tomography in Medical Diagnostics. Medical Infrared Imaging, CRC Press (2012)
41. Renkielska, A., Kaczmarek, M., Nowakowski, A., Grudzinski, J., Czapiewski, P., Krajewski, A., Grobelny, I.: Active dynamic infrared thermal imaging in burn depth evaluation. J. Burn Care Res. **35**, e294–e303 (2014)
42. Kaczmarek, M., Rogowski, J.: The role of thermal monitoring in cardiosurgery interventions. In: Bronzino, J.D., Peterson, D.R. (eds.) Biomedical Signals, Imaging, and Informatics. CRC Press (2014)

43. Moderhak, M., Nowakowski, A., Kaczmarek, M., Siondalski, P., Jaworski, Ł.: Active dynamic thermography imaging of wound healing processes in cardio surgery. In: Piętka, E., Kawa, J., Wieclawek, W. (eds.) Information Technologies in Biomedicine, vol. 4. Springer International Publishing, Cham (2014)
44. Kaczmarek, M., Nowakowski, A.: Analysis of transient thermal processes for improved visualization of breast cancer using IR imaging. In: Engineering in Medicine and Biology Society, 2003. Proceedings of the 25th Annual International Conference of the IEEE, pp. 1113–1116. IEEE (2003)
45. Kaczmarek, M., Nowakowski, A.: Active dynamic thermography in mammography. Task Quart. **8**, 259–267 (2004)
46. Nowakowski, A.: Limitations of active dynamic thermography in medical diagnostics. In: Engineering in Medicine and Biology Society, 2004. IEMBS'04. 26th Annual International Conference of the IEEE, pp. 1179–1182. IEEE (2004)
47. Amri, A., Saidane, A., Pulko, S.: Thermal analysis of a three-dimensional breast model with embedded tumour using the transmission line matrix (TLM) method. Comput. Biol. Med. **41**, 76–86 (2011)
48. Haifeng, Z., Liqun, H., Liang, Z.: Critical conditions for the thermal diagnosis of the breast cancer. In: Bioinformatics and Biomedical Engineering, 2009. ICBBE 2009. 3rd International Conference, pp. 1–3, 11–13 June 2009
49. Hu, L., Gupta, A., Gore, J.P., Xu, L.X.: Effect of forced convection on the skin thermal expression of breast cancer. J. Biomech. Eng. **126**, 204–211 (2004)
50. Jiang, L., Zhan, W., Loew, M.H.: Modeling static and dynamic thermography of the human breast under elastic deformation. Phys. Med. Biol. **56**, 187 (2011)
51. Ng, E.Y.K., Sudharsan, N.M.: An improved three-dimensional direct numerical modelling and thermal analysis of a female breast with tumour. Proc. Inst. Mech. Eng. [H] **215**, 25–37 (2001)
52. Sudharsan, N., Ng, E.: Parametric optimization for tumour identification: bioheat equation using ANOVA and the Taguchi method. Proc. Inst. Mech. Eng. [H] **214**, 505–512 (2000)
53. Sudharsan, N., Ng, E., Teh, S.: Surface temperature distribution of a breast with and without tumour. Comput. Methods Biomech. Biomed. Eng. **2**, 187–199 (1999)
54. Chen, M.M., Pedersen, C.O., Chato, J.C.: On the feasibility of obtaining three-dimensional information from thermographic measurements. J. Biomech. Eng. **99**, 58–64 (1977)
55. Chen, M.M., Holmes, K.R.: Microvascular contributions in tissue heat transfer. Ann. N. Y. Acad. Sci. **335**, 137–150 (1980)
56. Klinger, H.: Heat transfer in perfused biological tissue—I: general theory. Bull. Math. Biol. **36**, 403–415 (1974)
57. Wulff, W.: The energy conservation equation for living tissue. IEEE Trans. Biomed. Eng. **6**, 494–495 (1974)
58. Weinbaum, S., Jiji, L.: A new simplified bioheat equation for the effect of blood flow on local average tissue temperature. J. Biomech. Eng. **107**, 131–139 (1985)
59. Weinbaum, S., Jiji, L., Lemons, D.: Theory and experiment for the effect of vascular microstructure on surface tissue heat transfer—part I: anatomical foundation and model conceptualization. J. Biomech. Eng. **106**, 321–330 (1984)
60. Stańczyk, M., Telega, J.: Modelling of heat transfer in biomechanics-a review. P. 1. Soft tissues. Acta Bioeng Biomech. **4**, 31–61 (2002)
61. Arkin, H., Xu, L., Holmes, K.: Recent developments in modeling heat transfer in blood perfused tissues. Biomed. Eng. IEEE Trans. **41**, 97–107 (1994)
62. Zolfaghari, A., Maerefat, M.: Bioheat transfer. In: Bernardes, M.A.D.S. (ed.) Developments in Heat Transfer (2011)
63. Charny, C.K.: Mathematical models of bioheat transfer. Adv. Heat Transf. **22**, 19–155 (1992)
64. Khanafer, K., Vafai, K.: Synthesis of mathematical models representing bioheat transport. Adv. Numer. Heat Transf. **3**, 87 (2009)

65. Charny, C.K., Weinbaum, S., Levin, R.L.: An evaluation of the Weinbaum-Jiji bioheat transfer model for simulations of hyperthermia. In: Roemer, R.B., Mcgrath, J.J., Bowman, H.F. (eds.) Winter Annual Meeting of the American Society of Mechanical Engineers, pp. 1–10, 10–15 Dec. San Francisco, California, New York (1989)
66. Draper, J.W., Boag, J.: The calculation of skin temperature distributions in thermography. Phys. Med. Biol. **16**, 201 (1971)
67. Amalu, W.C., Hobbins, W.B., Head, J.F., Elliott, R.L.: Infrared imaging of the breast-an overview. In: Bronzino, J.D. (ed.) Biomedical Engineering Handbook, 3rd edn. CRC Press (2006)
68. Lahiri, B., Bagavathiappan, S., Jayakumar, T., Philip, J.: Medical applications of infrared thermography: a review. Infrared Phys. Technol. **55**, 221–235 (2012)
69. Ng, E.Y.K.: A review of thermography as promising non-invasive detection modality for breast tumor. Int. J. Therm. Sci. **48**, 849–859 (2009)
70. Winslow, C.-E., Gagge, A., Herrington, L.: Heat exchange and regulation in radiant environments above and below air temperature. Am. J. Physiol.-Leg. Content **131**, 79–92 (1940)
71. Mitchell, D., Wyndham, C., Hodgson, T., Nabarro, F.: Measurement of the total normal emissivity of skin without the need for measuring skin temperature. Phys. Med. Biol. **12**, 359 (1967)
72. Osman, M.M., Afify, E.M.: Thermal modeling of the normal woman's breast. J. Biomech. Eng. **106**, 123–130 (1984)
73. Gautherie, M., Quenneville, Y., Gros, C.: Metabolic heat production, growth rate and prognosis of early breast carcinomas. Biomedicine **22**, 328–336 (1975)
74. Gautherie, M.: Thermology of breast cancer: measurement and analysis of in vivo temperature and blood flow. Ann. N. Y. Acad. Sci. **335**, 383–415 (1980)
75. Priebe, L.: Heat transport and specific blood flow in homogeneously and isotropically perfused tissue. Physiol. Behav. Temp. Regul. 272–280 (1970)
76. Romrell L.J., Bland, K.I.: Anatomy of the breast, axilla, chest wall and related metastatic sites. Breast: Compr. Manag. Benign Malignant Dis. 22 (1998)
77. Ng, E.Y.K., Sudharsan, N.M.: Effect of blood flow, tumour and cold stress in a female breast: a novel time-accurate computer simulation. Proc. Inst. Mech. Eng. H. **215**, 393–404 (2001)
78. Amri, A., Pulko, S.H., Wilkinson, A.J.: Potentialities of steady-state and transient thermography in breast tumour depth detection: a numerical study. Comput. Methods Programs Biomed. **123**, 68–80 (2016)
79. De Cogan, D.: Transmission line matrix (TLM) techniques for diffusion applications. Gordon and Breach Science Publishers (1998)